

Identifying Decaying Supermassive Black Hole Binaries from their Variable Electromagnetic Emission

Zoltán Haiman¹, Bence Kocsis^{2,3}, Kristen Menou¹, Zoltán Lippai⁴, and Zsolt Frei⁴

¹ Department of Astronomy, Columbia University, New York, USA

² Harvard-Smithsonian Center for Astrophysics, Cambridge, USA

³ School of Natural Sciences, Institute for Advanced Study, Princeton, NJ, USA

⁴ Institute of Physics, Eötvös University, Budapest, Hungary

Abstract. Supermassive black hole binaries (SMBHBs) with masses in the mass range $\sim (10^4\text{--}10^7) M_\odot/(1+z)$, produced in galaxy mergers, are thought to complete their coalescence due to the emission of gravitational waves (GWs). The anticipated detection of the GWs by the future *Laser Interferometric Space Antenna (LISA)* will constitute a milestone for fundamental physics and astrophysics. While the GW signatures themselves will provide a treasure trove of information, if the source can be securely identified in electromagnetic (EM) bands, this would open up entirely new scientific opportunities, to probe fundamental physics, astrophysics, and cosmology. We discuss several ideas, involving wide-field telescopes, that may be useful in locating electromagnetic counterparts to SMBHBs detected by *LISA*. In particular, the binary may produce a variable electromagnetic flux, such as a roughly periodic signal due to the orbital motion prior to coalescence, or a prompt transient signal caused by shocks in the circumbinary disk when the SMBHB recoils and "shakes" the disk. We discuss whether these time-variable EM signatures may be detectable, and how they can help in identifying a unique counterpart within the localization errors provided by *LISA*. We also discuss a possibility of identifying a population of coalescing SMBHBs statistically, in a deep optical survey for periodically variable sources, before *LISA* detects the GWs directly. The discovery of such sources would confirm that gas is present in the vicinity and is being perturbed by the SMBHB – serving as a proof of concept for eventually finding actual *LISA* counterparts.

1. Introduction

The anticipated detection by *LISA* of gravitational waves emitted during the coalescence of supermassive black holes (SMBHs) in the mass range $\sim (10^4\text{--}10^7) M_\odot/(1+z)$ will constitute a milestone for fundamental physics and astrophysics. While the GW signatures themselves are a rich source of information, if the GW source produces electromagnetic (EM) radiation, and if the object can be securely identified in EM bands, this would open up entirely new scientific opportunities. The simultaneous study of photons and gravitons from a single source could probe fundamental aspects of gravitational physics [8, 15]. The GW sources can also be used as self-calibrated standard sirens [26], and cosmological parameters can be determined if the source redshift is identified [11, 13]. Finally, for many events in the above mass and redshift range, *LISA* will be able to measure the masses and spin vectors of the SMBHs, their

orbital parameters, and their luminosity distance, to a precision unprecedented in any other type of astronomical observation [17, 28]. If a counterpart is known, then the Eddington ratios and other attributes of black hole accretion physics can be studied in exquisite detail [13, 15].

Motivated by the above possibilities, several recent studies have addressed the question of whether finding a counterpart will be feasible, given *LISA*'s localization errors [11, 13, 14, 18, 15]. The crucial uncertainty, of course, is the nature (luminosity, spectrum, and time–evolution) of any EM emission produced by coalescing SMBHBs during the GW–inspiral stage. Such emission would have to be related to gas in the vicinity, and possibly accreting onto the coalescing SMBHBs. The gas around the BHs would likely settle into a rotationally supported, circumbinary disk. In a geometrically thin disk, the torques from the binary create a central cavity, nearly devoid of gas, within a region about twice the orbital separation [2] (for a nearly equal–mass binary), or a narrower gap around the orbit of the lower–mass BH in the case of unequal masses $q \equiv M_1/M_2 \ll 1$ and larger orbital separations [1]. In the latter case, the lower–mass hole could “usher” the gas inward as its orbit decays, producing a prompt and luminous signal during coalescence. In the former case, residual gas flow into the cavity and onto the BHs, such as suggested in numerical simulations [3, 20, 7], may still produce non–negligible EM emission. Around the time of coalescence, the gravitational waves shear the circumbinary gas and could brighten its emission detectably [16]. Finally, SMBHBs recoil at the time of their coalescence due to the emission of GWs, at speeds up to $4,000 \text{ km s}^{-1}$ (e.g. ref. [5] and references therein). The gas disk will respond promptly (on the local orbital timescale) to such a kick, which may produce prompt shocks, and transient EM emission after coalescence [19].[‡]

The complex processes involved in ultimately producing any EM emission remain poorly understood, and the level of the luminosity produced, as well as its spectrum and time–evolution, are essentially unknown. *However, any emission during and promptly following the inspiral stage is likely to be variable.* In this contribution, we discuss three issues related to using variability to identify EM counterparts. Can *LISA* events be localized to within the field of view of astronomical instruments (several deg^2), hours to weeks *prior* to coalescence (§ 2)? What is the response of the circumbinary gas to the gravitational recoil (“kick”) of the SMBHB at coalescence (§ 3)? Can we identify coalescing SMBHBs before the launch of *LISA*, as variable sources, due to periodic perturbations in the circumbinary gas (§ 4)?

2. Monitoring the 3D *LISA* Error Box Prior To Coalescence

The first and most fundamental question in searching for any EM counterpart by looking for variable emission, during the final stages of coalescence, is the accuracy to which the *LISA* source can be localized at various look–back times *prior to the coalescence*. (Coalescence is taken to occur when the binary separation reaches the innermost stable circular orbit; ISCO). Here we present time–dependent localization errors, obtained by the Harmonic Mode Decomposition method [14]. This technique uses the restricted, post–Newtonian approximation for the GW waveform, and applies the Fisher matrix technique to the Fourier transform of the waveform, to forecast parameter uncertainties. Orbits are assumed to be circular, and spins are neglected

[‡] Such brightening due to kick–induced disk heating can persist on much longer timescales, and could produce detectable emission – leading to recent proposals that this can help identify a population of such sources before *LISA*'s launch. This possibility will be briefly discussed further in § 4 below.

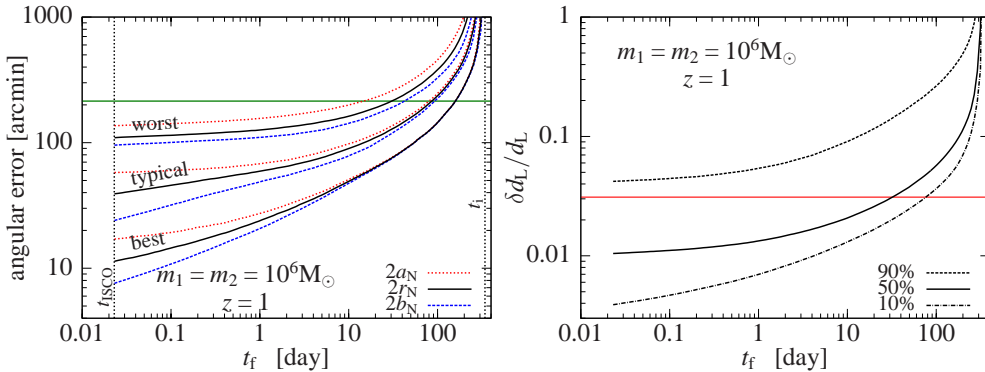


Figure 1. Evolution with pre-ISCO look-back time, t_f , of the expected LISA source localization uncertainties. *Left Panel:* Sky position errors (major axis $2a_N$, minor axis $2b_N$, and equivalent diameter, $2r_N \equiv 2\sqrt{a_N b_N}$, of the error ellipsoid). An equal-mass binary is shown as an example, with $M_1 = M_2 = 10^6 M_\odot$ at $z = 1$. Best, typical, and worst cases (among sources with random orientation) represent the 10%, 50%, and 90% levels of cumulative error distributions. The absolute errors are typically small enough to fit in the FOV of a wide-field instrument in the last few weeks, allowing a world-wide monitoring campaign. The horizontal line shows a diameter of 3.57° , which corresponds to localizing the source to within 10 deg^2 . *Right Panel:* Luminosity distance $d_L(z)$ errors for the same binary (10%, 50%, and 90% levels of cumulative error distributions as in the left panel). The horizontal line delineates the level of weak lensing uncertainties (adopted from ref. [13]). Knowing the luminosity distance to the accuracy of a few percent will allow the counterpart search to focus on candidates in a narrow redshift slice.

(this is justified until the last day or so of the merger; see [18]). The 17-dimensional parameter space describing the general binary inspiral is split into “slow” and “fast” parameters, based on the time-scales on which they modulate the waveform, and the two sets are assumed to be decoupled. The angular coordinates of the source, and its luminosity distance – representing the 3D localization of the source – are “slow” Fisher parameters, and information on these parameters are derived from the annual motion of *LISA* around the Sun. The reader is referred to [14] for a full list of assumptions and details about the method.

The time-evolving 1σ errors on the two-dimensional sky position are shown for an equal-mass binary, $M_1 = M_2 = 10^6 M_\odot$, at redshift $z = 1$ in Figure 1 (corresponding roughly to the optimal choice of mass/redshift combination; other masses and redshifts yield poorer localization). The HMD method, by construction, approximates the sky position errors by ellipses. Figure 1 shows the gradual improvement in localization, in the form of the major axis ($2a_N$), minor axis ($2b_N$) and equivalent diameter ($2r_N = \sqrt{4a_N b_N}$). Figure 1 displays results for three separate cumulative probability distribution levels, 90%, 50%, 10%, so that 10% refers to the best 10% of all events, as sampled by the random distribution of five angular parameters. The evolution of errors scales steeply with look-back time for $t_f \gtrsim 40$ days. For smaller look-back times, errors essentially stop improving in the “worst” (90% level) case, improve with a relatively shallow slope for the “typical” (50% level) case, and improve more steeply in the “best” case (10% level among the realizations of fiducial angular parameters). Similar evolutionary trends are seen for the luminosity distance $d_L(z)$ errors (shown in the right panel in Fig. 1).

Figure 2 displays contours of fixed “advance warning time” for typical (50%)

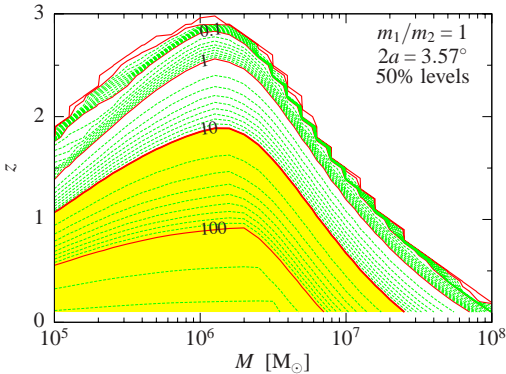


Figure 2. Contours of advance warning times in the total SMBHB mass (M) vs. redshift (z) plane, for typical events with SMBH mass ratio $q \equiv M_1/M_2 = 1$. The contours trace the look-back times at which the major axis ($2a$) of the localization error ellipsoid first falls below 3.57° . The contours are logarithmically spaced in days, and 10 days is highlighted with a thick curve.

events, adopting a 10 deg^2 FOV as a reference. The contours are logarithmically spaced, with solid contours every decade and the shaded region highlights the (M, z) region where at least 10-day advance notice will be available. This figure shows that 10 day advance warning to cover the full error ellipsoid with a single LSST pointing is possible for a range of masses and source redshifts, up to $M \sim 3 \times 10^7 M_\odot$ and $z \sim 1.7$.

The results shown in Figures 1 and 2 suggest that it will be possible to identify, prior to merger, a small enough region in the sky where any prompt electromagnetic (EM) counterpart to a LISA inspiral event will be located. Given sufficient advance notice, it will then be possible to trigger a world-wide monitoring campaign, to search for EM counterparts as the merger proceeds (and also during the most energetic coalescence phase).

The several square-degree field will, of course, contain a very large number of sources (a few $\times 10^5$ galaxies in total, at the limiting optical magnitude of ~ 27 mag that may be relevant; e.g. ref. [21] and discussion below). Having predictions for the spectrum and time-dependence of a coalescing SMBH binary, and therefore knowing what to look for, would obviously greatly help in identifying the counterpart, possibly allowing an identification even post-merger. Such a prediction, however, would require understanding the complex hydrodynamics and radiative properties of circumbinary gas at the relevant small separations of a few to a few thousand Schwarzschild radii. This is a notoriously difficult problem even in the much simpler case of steady accretion onto a single SMBH [22]. This suggests that the best strategy may be an “open-minded” search for any variable signatures prior and during coalescence.

There will be several ways, however, to cut down on the list of possible counterparts, using the photometric redshifts of the candidates (restricting the search to within a narrow, $\delta z \lesssim$ few percent, redshift slice; see the right panel in Fig. 1), the expected luminosity of the source, and the other parameters of the binary provided by *LISA* (for example, a variable EM signal may be much more likely if the spin and the orbital angular momenta are known to be aligned, as this may indicate the presence of circumbinary gas). These, and several other possible cuts are discussed further in ref. [15].

3. Prompt Shocks in the Gas Disk Around a Recoiling Binary

The recent break-through in numerical relativity has allowed a direct computation of the linear momentum flux (“kick”) produced during the coalescence of a SMBH binary. Such kicks may help produce *prompt* EM counterparts to GW sources detected by *LISA*. If the SMBHB is surrounded by a circumbinary gas disk, the disk will indeed respond promptly (on the local orbital timescale) to such a kick. If this results in warps or shocks, the disturbed disk could produce a transient EM signature [23]. As discussed above, the final sky localization uncertainty from *LISA* is typically a few tenths of a square degree, containing a large number of sources; monitoring this area for transient events *after* the merger may be another method to securely identify counterparts.

We investigated the response of a circumbinary disk to the kick [19]. We adopted the following simplified picture for the disk around a fiducial, equal-mass, $M_1 + M_2 = 10^6 M_\odot$ binary. The disk has an inner edge at $100r_S$ (Schwarzschild radii), inside which it is empty (with the gas evacuated due to torques from the binary; e.g. ref. [23]) and an outer edge at $10,000r_S$. Outside of this radius, there may still be gas, but it may be unstable to fragmentation, and it will, in any case, evolve slowly (the behavior of this gas will then not be relevant for a *LISA* counterpart search, but if emission is produced in this gas, it could help identify SMBHBs independently; see discussion in the next section). The scale-height and temperature at the inner edge is $h/r = 0.46$ and $T = 1.7 \times 10^6 \text{K}$, respectively. The scale-height remains constant with radius out to $2,000r_S$, beyond which it increases nearly linearly ($h \propto r^{21/20}$). The temperature varies with radius as $T \propto r^{-9/10}$ (see ref. [19] for further details).

The important features of such a disk (as well as other proposed variants of thin α -disks) are the following: (i) orbital motions in thin disks are supersonic, so that the gas is susceptible to shocks if disturbed; (ii) at the relevant radii outside $100r_S$ the viscous time-scale is long, and the orbits are near Keplerian; (iii) gas near the inner edge of disk is tightly bound to the kicked BHB ($v_{\text{orbit}} \sim 2.1 \times 10^4 \text{ km s}^{-1}$), but the outer edge ($v_{\text{orbit}} \sim 2.1 \times 10^3 \text{ km s}^{-1}$) can be marginally bound, or even unbound, for large kicks (a rough condition for being bound is $v_{\text{orbit}} \gtrsim v_{\text{kick}}$), and (iv) the total disk mass within $10,000r_S$ is much less than the BHB mass, which justifies ignoring the inertia of the gas bound to the BHB.

For a quantitative assessment of the disk’s response to the kick, we employed the following approximation: the disk particles are assumed to be massless, collisionless, and initially on co-planar, circular orbits. The kick simply adds the velocity \vec{v}_{kick} to the instantaneous orbital velocity of each particle (in the inertial frame centered on the BHB). We used $N = 10^6$ particles, distributed randomly and uniformly along the two-dimensional surface of the disk. The kick velocity was varied between $500 \text{ km s}^{-1} < v_{\text{kick}} < 4,000 \text{ km s}^{-1}$, and directed either perpendicular or parallel to the initial disk plane. Note that in both the perpendicular and parallel case, we start with a two-dimensional particle distribution (i.e. an infinitely thin disk), but in the perpendicular case, we then follow the orbits in 3D.

Figure 3 shows, as an example, a face-on view of the surface density of the disk 90 days after a kick with $v_{\text{kick}} = 500 \text{ km s}^{-1}$ in the plane of the disk (left panel). The sharp, tightly wound spiral features clearly seen in the figure trace the locus of points where particles cross each other, corresponding formally to a density caustic. The spiral caustic first forms at ~ 30 days, and then propagates outward at a speed of $\approx 500 \text{ km s}^{-1}$, so that the outermost caustic at time t_c is located at $r_c \sim t_c v_{\text{kick}}$

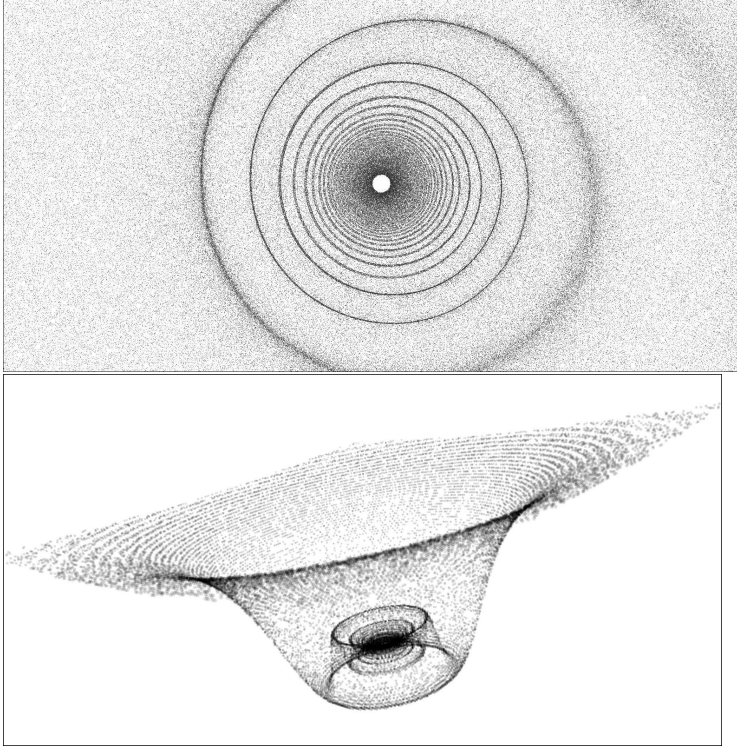


Figure 3. *Top Panel:* The top view of the surface density of a disk around an $M_1 + M_2 = 10^6 M_\odot$ BH binary, which recoiled within the disk plane at the velocity of $v_{\text{kick}} = 500 \text{ km s}^{-1}$, oriented vertically upward in the diagram. The disk is initially assumed to have an inner edge at $r_{\text{in}} = 100r_S$ (Schwarzschild radii), and is shown here out to a radius of $r_{\text{in}} = 5,000r_S$, at a time $t = 90$ days after the kick. A tightly wound, outward-moving spiral caustic develops in about a month. The dark/light shades correspond to regions of high/low density, the low-density regions being similar to the initial surface density, and the high-density regions about 10 times overdense. *Bottom Panel:* Aerial view of a disk with a kicked SMBHB, as in the left panel, except here the kick is oriented perpendicular to the disk, and the snapshot is taken at $t = 1$ week. For visual clarity, the graphic contrast was increased relative to the left panel, and the diagram stretched by a factor of 10 along the axis perpendicular to the disk plane. The density distribution is azimuthally symmetric, and while there are mild concentric density fluctuations, strong enhancements (i.e. caustics) were found to develop only after a delay of \approx one year.

(this behavior can be roughly understood using epicycles; refs. [19, 25]). The right panel in Figure 3 shows, for comparison, the aerial view of the 3D particle density one week after a kick with the same velocity, but perpendicular to the disk. The density profile in this case remains azimuthally symmetric, but still develops concentric rings of density fluctuations (although we find the density enhancements are much weaker, at the ten percent level).

These results suggest that strong density enhancements can form promptly after a supersonic kick in the plane of the circumbinary disk, within a few weeks of the coalescence of a $\sim 10^6 M_\odot$ BHB. Because the disk is cold, and caustics are formed when particles first cross each other along their orbits, this implies that corresponding shocks could occur in a gas disk. For hydrodynamical shocks to occur within a

finite-pressure gas, the relative motions v_c between the neighboring particles that produce the caustic must exceed the sound speed. At the outermost radius where the disk is marginally bound to the BHB, one expects $v_c \sim v_{\text{kick}} \sim v_{\text{orbit}}$; relative motions will be slower further inside. The relative speed should roughly correspond to covering the epicyclic amplitude $\sim (v_{\text{kick}}/v_{\text{orbit}})r_c$ in the caustic-formation time $t_c \sim r_c/v_{\text{kick}}$, yielding $v_c \sim v_{\text{kick}}^2/v_{\text{orbit}}$. For $v_{\text{kick}} = 500 \text{ km s}^{-1}$, this predicts $v_c \sim 25 \text{ km s}^{-1}(r/1000r_S)^{1/2}$; we have verified in our simulations that particles cross the caustics at speeds within $\sim 30\%$ of this predicted value. Compared with the sound speed $c_s \approx 25 \text{ km s}^{-1}(r/1000r_S)^{-9/20}$, this suggests that the density waves produced by the kick in the gas beyond $\sim 700r_S$ will indeed steepen into shocks. We also found that the inclination of the kick may be important in determining the strength and timing of such shocks.

The nature of the emission resulting from the shocks or density enhancements will have to be addressed in future work, by incorporating the effects of hydrodynamics, computing the heating rate at the location of the spiral shocks, and modeling the overall disk structure and vertical radiation transport.[§] However, in the fiducial case discussed above, if we assume that the shocked gas is heated to temperatures corresponding to v_c , and t_c is the time-scale on which the corresponding thermal energy is converted to photons, then we find that the luminosity may be a small but non-negligible fraction, 0.2 percent to 5 percent of the Eddington luminosity of the central BH, and would increase with time roughly as $L_{\text{kick}} \propto t^2$. This suggests that the afterglows may be detectable, at least for nearby BHs and/or for the most massive BHs in LISA’s range (which extends up to $M_{\text{bh}} \approx 10^7 M_\odot$). We may also speculate on the spectral evolution of the “kick after-glow”, based on the characteristic shock velocity at each radius. We find that the luminosity is dominated by the outermost shocked shells, with the spectrum peaking at the characteristic photon energy corresponding to $kT_{\text{shock}} \propto v_c^2 \propto v_{\text{orbit}}^{-2} \propto r$. The shocks could therefore result in an afterglow, starting from $700r_S/v_{\text{kick}} \sim 50$ days, first peaking in the UV band ($\sim 3\text{eV}$ or $\sim 0.3\mu\text{m}$, corresponding to $\sim 25 \text{ km s}^{-1}$), and then hardening to the EUV/soft X-ray ($\sim 50\text{eV}$) range after \sim two years. The detection of such an afterglow would help identify EM counterparts to *LISA* events.

4. Searching for Gravitational Binary Inspirals Before LISA

Numerical simulations suggest that the central cavity of the circumbinary disk is not completely empty, and that there can be non-negligible gas inflow into this cavity from the outside disk [3, 20, 7]. The perturbations of the circumbinary gas by the rotating quadrupole potential of the binary, in fact, appears to impose large fluctuations on this inflow rate, tracking the orbital period [20, 7]. We must emphasize that the level and nature of EM emission, associated with this inflow (or with other effects from the gas in the vicinity of the binary during the late stages of binary evolution), remains essentially unknown. Furthermore, even in the most optimistic scenario, in which a clearly periodic emission is indeed produced, at a significant and detectable flux level, there remains the (potentially severe) observational challenge of distinguishing such variability from other possible sources of periodic variations.

Despite these uncertainties and caveats, however, it is interesting to ask the

[§] Our preliminary work, based on hydrodynamical simulations, does indicate that gas disks with realistic pressure profiles still develop strong shocks [6].

following question: if, indeed, non-negligible emission is produced during the late stages of binary evolution, and the luminosity varies periodically on the orbital time-scale, could such periodic sources possibly be identified in EM surveys, even before *LISA* becomes operational?

As the orbit of each individual binary shrinks, its orbital period, and therefore, by assumption, its variability timescale decreases. The evolution of a binary embedded in a thin circumbinary disk generically proceeds through three distinct stages (see ref. [10]). (i) First, the binary is strongly coupled to the circumbinary disk and is driven by viscosity (analogous to “disk-dominated” planetary migration), and the radius of the gap follows the binary. As the binary separation shrinks below $\sim 10^5 r_S$ ($10^3 r_S$) for mass ratios $q \equiv M_1/M_2 \sim 1$ ($q \sim 0.01$), the local disk density starts to dominate over the binary mass, and the binary evolves more slowly, according to so-called “secondary-dominated” Type-II migration. During this stage, the GW emission is negligible. (ii) Later, within the radius $\sim 500 r_S$, the binary starts to be driven primarily by GWs but the radius of the gap can still follow the binary. (iii) Finally, within $\sim 100 r_S$ the binary is entirely driven by GWs and the binary falls in much more quickly than the outer edge of the gap is able to move inward. The ordering of these events is valid for a very broad range of binary and disk parameters. Note that the outcome of the gas inside the binary’s orbit is left unspecified above (see ref. [1] for a possible outcome for $q \ll 1$).

In the last, GW-driven regime, the binary spends a characteristic time T_{GW} at each orbital separation $r_{\text{orb}} < r_{\text{GW}}$ that scales with the corresponding orbital time as $T \propto t_{\text{orb}}^{8/3}$. The incidence rate of sources that have similar inferred BH masses, and show near-periodic variability on the time-scale $t_{\text{var}} \approx t_{\text{orb}}$, would then follow $N \propto t_{\text{var}}^{8/3}$. On the other hand, at larger separations, where the evolution is due to viscous processes, the incidence rate has a much flatter dependence. For near-equal mass binaries, the scaling is between $N \propto t_{\text{var}}^{25/51}$ and $N \propto t_{\text{var}}^{7/12}$, depending on whether the opacity is dominated free-free absorption or electron scattering, respectively. For $q \ll 1$, the scaling is slightly steeper, between $N \propto t_{\text{orb}}^{5/6}$ and $N \propto t_{\text{orb}}^{14/15}$ for free-free absorption or electron scattering opacity, respectively (see the Appendix in ref. [10]). In the left panel of Figure 4, we show that the time spent at each orbital period can be interestingly long, i.e. a non-negligible fraction of the expected lifetime of quasar activity of a $\sim \text{few} \times 10^7$ years.

Can we detect the flux variations from these sources? Luminosity variations corresponding to a fraction $f_{\text{Edd}} \lesssim 0.01$ of the Eddington luminosity (or, e.g., a periodic component with amplitude $i \approx 26 + 2.5 \log[(f_{\text{Edd}}/0.01)(M_{\text{BH}}/3 \times 10^7 M_{\odot})^{-1}]$ magnitudes in the optical for BHs at $z = 2$) would have not been found in existing variability surveys. However, as shown in Figure 4, a dedicated, deep survey of a $\sim \text{deg}^2$ area, possibly with existing instruments, could detect a population of \sim several to \sim several thousand such “transition sources” with a range of periods between 20 weeks $\lesssim t_{\text{var}} \lesssim 60$ weeks. In the right panel of Figure 4, we use the luminosity function of optical quasars, and assume that each optical quasar results from a SMBH–SMBH merger, and, as the binary orbit decays, it goes through the evolutionary stages discussed above (see ref.[10] for more details). The figure then shows the required depth and area coverage for a multi-year survey to detect such periodic sources, covering a factor of three range in period. The dependence in the abundance of these sources on their period – in particular, a switch from a flat, viscosity-driven power-law between $N \propto t_{\text{var}}^{1/2}$ and $N \propto t_{\text{var}}^1$, to the much steeper, GW-driven $N \propto t_{\text{var}}^{8/3}$ – below

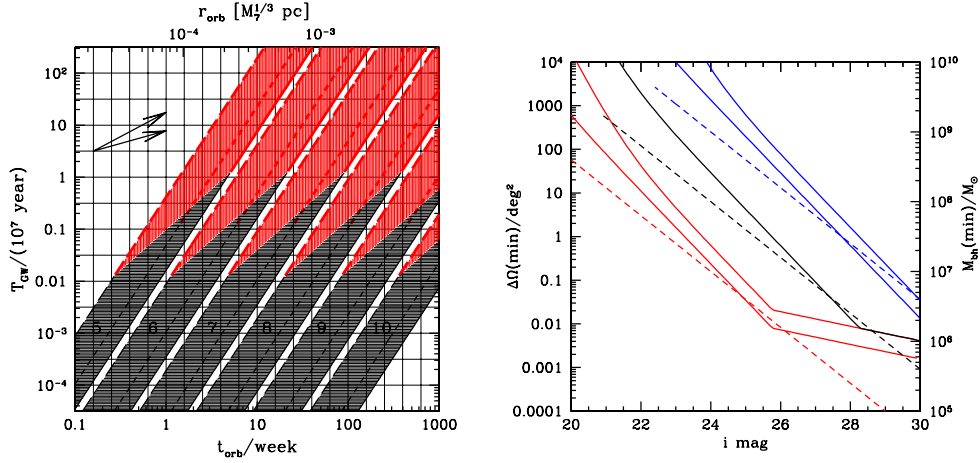


Figure 4. *Left Panel:* The figure shows the time T_{GW} that a SMBHB, whose coalescence is driven entirely by gravitational radiation, spends at a radius where the orbital time is within t_{orb} . Both T_{GW} and t_{orb} are in redshifted units (as measured on Earth). Each of the shaded regions corresponds to a different total BH mass ($[1+z]M_{\text{tot}} = [10^{5,6,7,8,9,10}]M_{\odot}$; top to bottom), and shows three different mass ratios ($q = [1, 0.1, 0.01]$; bottom to top, or solid, short-dashed, and long-dashed, respectively). The quantity on the y axis can be interpreted as the duty-cycle for each source during which it exhibits periodic variability on the time-scale $t_{\text{var}} \approx t_{\text{orb}}$. The thick (red) portion of the lines and the vertically shaded (red) areas indicate the orbital separations, for each mass, where binary evolution may no longer be dominated by GWs. The slope of the arrows indicate the flatter evolution of the binary when it decays due to viscous torques: the flatter arrow corresponds to the slope $T \propto t_{\text{orb}}^{25/51}$ for near-equal mass binaries, and the slightly steeper arrow to $T \propto t_{\text{orb}}^{14/15}$ for $q \ll 1$ (see Appendix in ref. [10] for details). For reference, the x axis labels on the top show the orbital radius corresponding to each orbital time; for $M = 10^7 M_{\odot}$ (or $M_7 = 1$) and $z = 0$, the plotted range covers $1.6 \times 10^{-5} - 7.5 \times 10^{-3}$ pc, or 17-77,000 Schwarzschild radii.

Right Panel: This panel shows the sky coverage of a future survey, required to find at least one periodic source, with a period of at most 20 weeks, as a function of the i -band magnitude limit on the variable component. This will ensure that a multi-year survey, could find many more sources with longer periods, e.g. periods up to 1 year, demonstrating the periodic nature of the variations, and allowing to deduce the abundance of periodic sources as a function of period. The three solid curves show results assuming that the variable component is a fraction 0.3, 0.03, and 0.003 of the Eddington luminosity of the binary. Each dashed curve shows the corresponding mass of the SMBHB of which there would be a single example of a $t_{\text{var}} = 20$ -week periodic variable in the survey (~ 20 sources with the same luminosity are then predicted with a $t_{\text{var}} = 60$ week period in the same survey volume, assuming pure GW-driven evolution, or fewer such longer-period sources, if viscosity speeds up the evolution significantly).

a characteristic $t_{\text{var}} \sim$ tens of weeks (corresponding to $\sim 10^3$ Schwarzschild radii for equal-mass $\sim 10^6 M_{\odot}$ binaries), could confirm (i) that the orbital decay for sources below a characteristic t_{var} is indeed driven by GWs and (ii) also that circumbinary gas is present at small orbital radii and is being perturbed by the BHs – serving as a proof of concept for eventually finding actual *LISA* counterparts.

Finally, we mention two other possibilities to identify coalescing SMBHBs before *LISA*'s launch. First, [24] and [25] followed the response of the gas disk around a recoiling SMBHB, similar to our calculation described in § 3, but on much longer timescales ($\sim 10^4$ years). Ref. [24] found that the shocked gas, thrown out of the disk plane by an oblique kick, may produce bright flares in X-ray lines (assuming it remains optically thin). Ref. [25], on the other hand, assumed that the disk gas is optically thick, and that the shocks are promptly dissipated in the disk plane, and derived a characteristic infrared light-curve. The above effects arise from the change in the gravitational potential, following the recoil, i.e. from the “shaking” of the disk. A different possibility is that once the BHs have merged, the torques from the rotating quadrupolar potential cease to act on the gas outside the inner cavity, allowing the gas to accrete onto the merged binary on the viscous time-scale [23]. An X-ray “afterglow” may then occur after a delay of $\sim 7(1+z)(M/10^6 M_\odot)^{1.32}$ years. This could be detectable in *LISA* follow-up observations, or perhaps without a *LISA* trigger for very massive BHs at high z , where the time-scale is long.

Acknowledgments

ZH thanks the organizers of the conference. The work described here was supported by NASA (grant NNX08AH35G), and by the Polányi Program of the Hungarian National Office for Research and Technology (NKTH).

References

- [1] P. J. Armitage, & P. Natarajan, *Astrophys. J.* **567**, L9 (2002).
- [2] P. Artymowicz, & S. H. Lubow, *Astrophys. J.* **421**, 651 (1994).
- [3] P. Artymowicz, & S. H. Lubow, *Astrophys. J. Lett.* **467**, L77 (1996).
- [4] J. E. Barnes, & L. Hernquist, *Ann. Rev. Ast. & Astrophys.* **30**, 705 (1992).
- [5] M. Campanelli, et al., *Phys. Rev. Lett.* **98**, 231102 (2007).
- [6] L. Corrales, A. MacFadyen, & Z. Haiman, *Astrophys. J.*, to be submitted (2008).
- [7] J. Cuadra, P. J. Armitage, R. D. Alexander, & M. C. Begelman, *Mon. Not. Royal Ast. Soc.*, submitted; arXiv:0809.0311
- [8] C. Deffayet, & K. Menou, *Astrophys. J.* **668**, L143 (2007).
- [9] A. Escala, R. B. Larson, P. S. Coppi, & D. Mardones, *Astrophys. J.* **607**, 765 (2004).
- [10] Z. Haiman, B. Kocsis, & K. Menou, *Astrophys. J.*, submitted; arXiv:0807.4697
- [11] D. E. Holz, & S. A. Hughes, *Astrophys. J.* **629**, 15 (2005).
- [12] P. B. Ivanov, J. C. B. Papaloizou, & A. G. Polnarev, *Mon. Not. Royal Ast. Soc.* **307**, 79 (1999).
- [13] B. Kocsis, Z. Frei, Z. Haiman, & K. Menou, *Astrophys. J.* **637**, 27 (2006).
- [14] B. Kocsis, Z. Haiman, K. Menou, & Z. Frei, *Phys. Rev. D* **76**, 022003 (2007).
- [15] B. Kocsis, Z. Haiman, & K. Menou, *Astrophys. J.* **684**, 870 (2008).
- [16] B. Kocsis, & A. Loeb, *Phys. Rev. Lett.* **101**, 041101 (2008).
- [17] R. N. Lang, & S. A. Hughes, *Phys. Rev. D* **74**, 122001 (2006).
- [18] R. N. Lang, & S. A. Hughes, *Astrophys. J.* **677**, 1184 (2008).
- [19] Z. Lippai, Z. Frei, & Z. Haiman, *Astrophys. J. Lett.* **676**, L5 (2008).
- [20] A. MacFadyen, & M. Milosavljević, *Astrophys. J.* **672**, 83 (2008).
- [21] P. Madau, “Cosmic Star Formation History and the Brightness of the Night Sky”, in *From Extrasolar Planets to Cosmology: The VLT Opening Symposium*, edited by J. Bergeron and A. Renzini (Springer-Verlag, 2000), p. 52.; arXiv:astro-ph/9907268
- [22] F. Melia, & H. Falcke, *Ann. Rev. Ast. & Astrophys.* **39**, 309 (2001).
- [23] M. Milosavljevic, & E. S. Phinney, *Astrophys. J.* **622**, L93 (2005).
- [24] G. A. Shields, & E. W. Bonning, *Astrophys. J.* **682**, 758 (2008).
- [25] J. D. Schnittman, & J. H. Krolik, *Astrophys. J.* **684**, 835 (2008).
- [26] B. F. Schutz, *Nature* **323**, 310 (1986).
- [27] J. H. Taylor, & J. M. Weisberg, *Astrophys. J.* **253**, 908 (1992).
- [28] A. Vecchio, *Phys. Rev. D* **70**, 042001 (2004).